

Primljen / Received: 26.2.2018.
Ispravljen / Corrected: 21.8.2018.
Prihvaćen / Accepted: 3.9.2018.

Dostupno online / Available online: 10.10.2018.

Remediation of traditional stone columns by lead inlays

Authors:



Assit.Prof. **Josip Atalić**, PhD. CE
University of Zagreb
Faculty of Civil Engineering
Department for Engineering Mechanics
atalic@grad.hr



Assit.Prof. **Mario Uroš**, PhD. CE
University of Zagreb
Faculty of Civil Engineering
Department for Engineering Mechanics
uros@grad.hr



Assit.Prof. **Marta Šavor Novak**, PhD. CE
University of Zagreb
Faculty of Civil Engineering
Department for Engineering Mechanics
msavor@grad.hr

Original scientific paper

Josip Atalić, Mario Uroš, Marta Šavor Novak

Remediation of traditional stone columns by lead inlays

Typical cracks often occur on traditional stone columns at the position of joints. In addition, such columns bear witness of various repair methods that have been used over time to stop continuous spreading of cracks. Systematic numerical and laboratory analyses conducted on almost real size samples have revealed that the basic cause of cracking is the concentration of stress at contact surfaces. Some laboratory testing and numerical analysis results, relating to the traditional form of repair with lead inlay placed between column parts, are presented in the paper.

Key words:

stone column, contact stress, uneven surface, stress concentration, lead inlay, laboratory testing, numerical analysis

Izvorni znanstveni rad

Josip Atalić, Mario Uroš, Marta Šavor Novak

Sanacija tradicijskih kamenih stupova olovnim umetkom

Na tradicijskim kamenim stupovima često se mogu uočiti karakteristične pukotine u području spojeva, ali i različite načine sanacija kojima se pokušavalo zaustaviti njihovo kontinuirano širenje. Sustavnim je numeričkim i laboratorijskim analizama na gotovo realnim dimenzijama uzoraka kao temeljni uzrok raspucavanja orkrivena koncentracija naprezanja na kontaktnim plohama. U radu je prikazan dio rezultata laboratorijskih ispitivanja i numeričkih analiza tradicijskoga oblika sanacije s olovnim umetkom postavljenim između dijelova stupa.

Ključne riječi:

kameni stup, kontaktno naprezanje, neravna ploha, koncentracija naprezanja, olovni umetak, laboratorijska ispitivanja, numerička analiza

Wissenschaftlicher Originalbeitrag

Josip Atalić, Mario Uroš, Marta Šavor Novak

Sanierung von traditionellen Steinsäulen durch Bleieinsätze

An traditionellen Steinsäulen sind häufig charakteristische Risse im Fugenbereich zu erkennen, aber auch unterschiedliche Arten der Sanierung, mit denen man deren kontinuierliche Ausdehnung aufzuhalten versuchte. Durch systematische numerische und labortechnische Analysen an nahezu realistischen Probeabmessungen entdeckte man als grundlegende Ursache für das Absplittern die Spannungskonzentration an den Kontaktflächen. In der Abhandlung wird ein Teil der Ergebnisse der Laboruntersuchungen und der numerischen Analysen der traditionellen Form der Sanierung mit Bleieinsätzen dargelegt, die zwischen den Säulenteilen eingesetzt werden.

Schlüsselwörter:

Steinsäule, Kontaktspannung, unebene Fläche, Spannungskonzentration, Bleieinsatz, Laboruntersuchungen, numerische Analyse

1. Introduction

An initial motive for an extensive study of traditional stone columns has stemmed from continuous problems with columns in the atrium of the Rector's Palace in Dubrovnik where, after numerous retrofits over the centuries, the main cause of the problem has still not been discovered, nor the fracture propagation has been stopped. On top of that, historic reports have often placed emphasis on a structural deficiency, i.e. on "permanent phenomena that cause damage to columns" [1]. The problem of cracking of traditional columns has been observed all over Croatia [2], but has also been registered worldwide [3] on a wide variety of traditional columns [4]. Throughout the history, various retrofit techniques have been used, and so previous interventions can now often be observed on columns: various stirrups, inserts, and connections for linking column elements, filling of gaps, replacement of individual elements, etc. (Figure 1). The basic idea behind such interventions was to prevent fracture propagation as, otherwise, it would endanger the safety (detachment and fall of elements) and, in the end, can result in column collapse. The objective of this study is to grasp the very core of the problem, i.e. to mitigate the structural deficiency itself (arising from initial structural concepts from historic reports) and hence to prevent or at least postpone further fracturing of columns for a longer period of time.

Various traditional stone columns have frequently been used by builders, especially with regard to column slenderness. This paper focuses on traditional columns (Figure 2.a) composed of the body, base and capital, which were usually joined together by an iron dowel (placed into openings of a somewhat greater diameter that were subsequently filled with lead), while contact surfaces were carefully smoothed down and joined together (Figure 1). It is obvious that this type of connection was mostly used as a means to transmit centric load, i.e. it was not capable of transmission significant eccentric loads, which is in line with the concept of structural systems that was normally used in historic buildings. In addition, it is important to note that columns, although in most cases the most slender elements, were very rarely highly stressed while horizontal load (such as the load generated by earthquakes) was in most cases resisted by walls. However, when subjected to earthquake action, columns have to follow displacements of the structure, which

causes disturbance in the transfer of compressive forces along the column elements, especially at contact surfaces (which detach from one another). Other actions, such as imperfections during construction, settlement of foundations, redistribution of stress in vaults, temperature, changes occurring over extended periods of time, etc., may also cause the deviation or eccentricity of the thrust line. Loads, such as in current research [6] shows that even smaller eccentricities in thrust line cause relative rotation of column parts, i.e. the opening of the joint on one side and leaning of the contact to the other side (Figure 2.c), which causes significant stress concentration (Figure 2.d), and opening of typical fractures in the vicinity of such contacts. Moreover, it has been demonstrated that a cracked condition is very sensitive to load changes, such as temperature or live load, which contributes to progressive fracture propagation [7]. Finally, in most cases the columns should not be highly utilized for vertical and horizontal loads, but it has been shown that local stress concentrations at contact surfaces are sufficient to cause fractures on many columns. The concentrations are primarily caused by thrust line deviations, but current research has shown that unavoidable irregularities of contact surfaces, preventing uniform contact, must also be taken into account [5].

It should be noted that the problem of stress concentration at contact areas remains in many cases undetected or is not even taken into account. It is difficult to identify this problem by traditional calculations, using for instance approximate graphical methods, and by selecting usual relationships between structural elements [8] or the compression-tension analogy, simply because the displacements are very small. On the other hand, global structural models that are most often used in modern numerical calculations [9] cannot adequately cover complex behaviour of small details, especially in the post-critical region (where many specific data are required). Furthermore, common experimental tests, involving determination of axial force levels in columns of historic buildings, are normally not conducted in the vicinity of contacts, and may lead researchers to totally wrong conclusions, as stress concentrations are already distributed (Figure 2.d). That is why the analyses of historic buildings that do not involve a detailed approach to joints/connections may strongly underestimate the utilization of columns and hence of the entire structures, as has been confirmed by previous investigations [5].

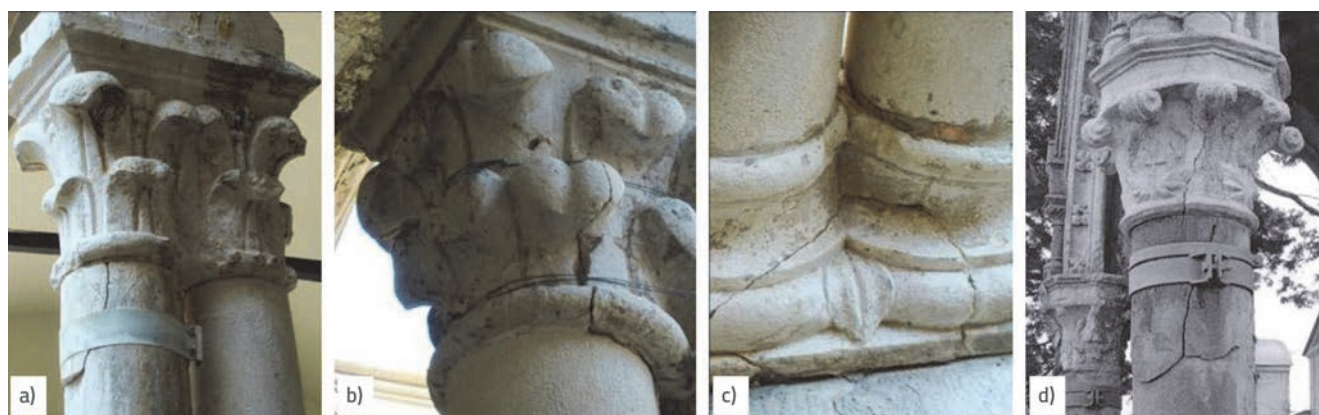


Figure 1. Fractures on traditional stone columns with traces of previous retrofit strategies [5]

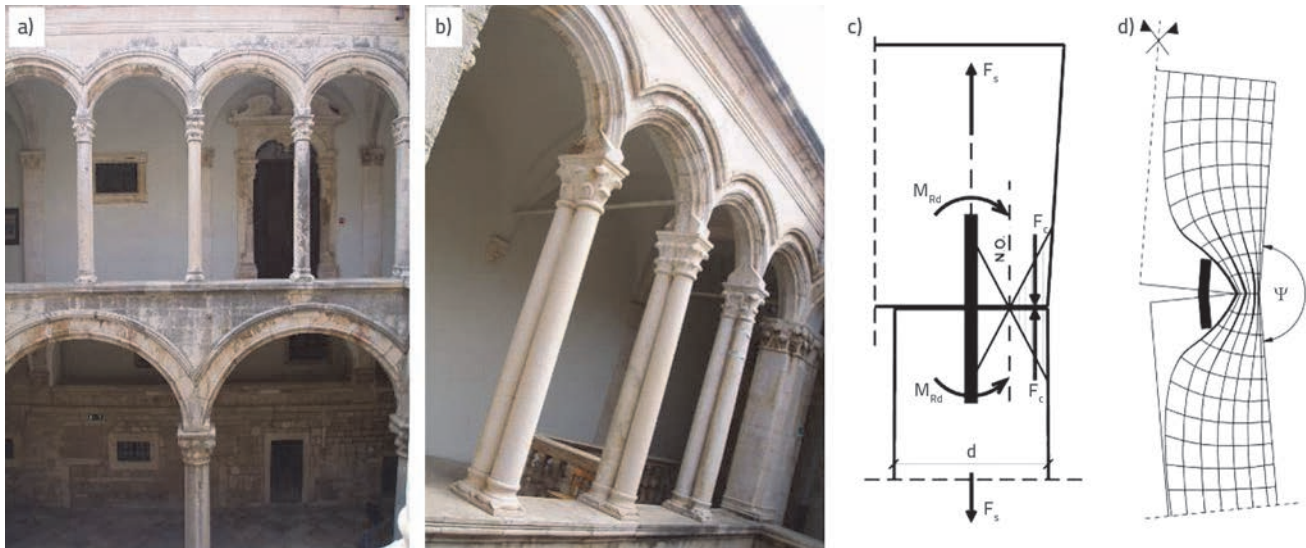


Figure 2. a) Traditional stone columns; b) coupled columns on the first floor of the Rector's Palace in Dubrovnik; c) Connection behaviour model with internal forces and stresses [7]; d) Distribution of stress trajectories [6]

Although cracks are frequently found in historic buildings, they are most often not critical as numerous load redistributions are possible through proper design of such buildings. However, in case of columns, this redistribution is limited (small cross-section), so local instabilities can form quite rapidly as a result of local column fracturing [10]. Retrofit activities can prevent full cracking of columns (example of Rector's Palace), but the problem (structural deficiency) remains, and, after retrofit, columns are affected again by the same fracturing process. Causes of problems with traditional columns have been investigated in several phases. This paper is a direct follow-up of earlier research efforts, especially of the research conducted in [5] where a detailed numerical and experimental analysis of the influence of contact stresses on bearing capacity of columns is given, and these stresses are defined as one of principal causes of cracking. Using assumptions from the above mentioned investigations and premises resulting from laboratory testing described in [5], this paper presents results of a retrofit method involving placing a lead insert (inlay) between parts of a column. Because of its properties, a lead insert can be used to compensate the described problems occurring on contact surfaces, i.e. it can actually prevent stress concentrations. The described retrofit method has been found acceptable by the multidisciplinary team of experts that usually cooperates in retrofit activities relating to historic structures and, if we add that the lead insert is almost invisible (as it is placed between column elements) and that the intervention is reversible, this retrofit method can also be considered compliant with modern recommendations [11]. The basic motivation is to keep the original concept of the structure (including all load-bearing elements) and to reduce difficulties relating to contact stress concentrations. It should however be noted that the retrofit with lead inserts is just one among numerous possibilities because modern procedures enable better elaboration of details. A particular emphasis should be placed on experimental research [12] involving analysis of various contact-surface connection possibilities. It is reasonable to believe

that the study of various stone column retrofit alternatives will also be pursued in the future, as historic buildings are structures of inestimable value.

2. Laboratory testing

2.1. Laboratory testing setup

Laboratory tests are crucial for interpreting behaviour of joints, especially because many input parameters that are encountered in the analysis of historic structures are not sufficiently reliable. The problem is far from negligible because destructive test methods usually are not permitted in case of historic buildings [10]. Testing setup used in an earlier phases of study, which focused on the influence of centric and eccentric load on contact stresses, was adopted also for the this lead inlay testing [5]. The testing setup, described in full detail in [5], will only briefly be described in this paper, i.e. as needed for the purposes of analysis and presentation of results.

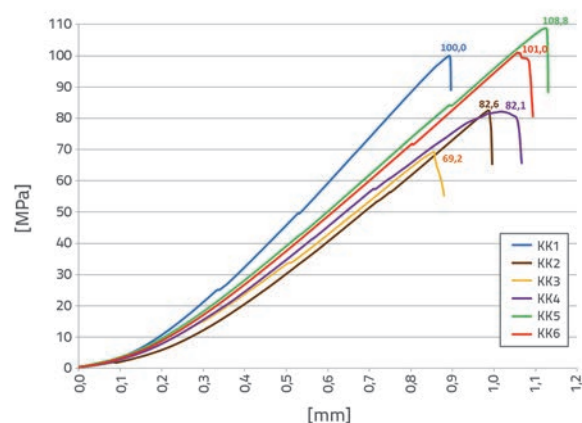


Figure 3. Compressive strength diagram

The samples are made of stone type Korunito originating from the Piska quarry, situated on the Island of Korčula. When taking samples, special attention was paid to their extraction (depth and orientation of layers, water traces, level of damage, etc.) and final treatment. Mechanical properties of stone were determined by testing compressive strength, bending strength, modul of elasticity, and fracture mechanics parameters. Compressive strength results for samples measuring 5.0 x 5.0 x 5.0 cm are presented in Figure 3, while a detailed presentation of experimental results can be found in [13].

The test procedure developed for this purpose (Figure 4) involves application of load through a steel beam, because numerical checks and comparison between results of three-dimensional numerical model of the existing structure (Figure 16.a) and test model results (Figure 16.b) have revealed that this procedure is the most appropriate. The basic intent was to closely simulate behaviour of existing structures, i.e. to ensure highly realistic distribution of stresses affecting the column. In addition, the load application region had to be moved away from contact surfaces, and proper attention had to be paid to testing safety, controlled application of force, simple assembly, laboratory constraints, etc. The steel beam (Figure 4) is specially adapted for application of load using the universal compression/tension machine Zwick/Roell with two hydraulic pistons, one of which (± 600 kN in capacity) was placed on the beam above the column (centrally) and the other (approximately 250 kN in capacity) was placed in the middle of the steel beam length (eccentrically). During the testing procedure, the force level was applied by displacement control with increments of 0.01 mm/s, which is significant for monitoring post-critical behaviour of the connection, i.e. for defining residual bearing capacity at cracking. The relative rotation of column elements, i.e. the pressure of the capital exerted on one side of the column cross section, was obtained by bending of the steel beam and by fixed connection between the beam and the capital (realized using four bolts in epoxy resin) (Figure 2.c and Figure 16.b). Sample dimensions were selected based on coupled columns constructed at the storey of the Rector's Palace in Dubrovnik (Figure 2.b). The capital (measuring

300 mm in diameter, and 500 mm in height) was placed onto the column ($d = 250$ mm, $h = 1500$ mm) and the two were connected with a steel dowel ($d = 16$ mm, $h = 150$ mm) placed in openings ($d = 19$ mm, $h = 100$ mm) in the centre of cross-section. The column was similarly connected to the base ($d = 300$ mm, $h = 200$ mm), which rested on the steel pedestal [5]. The height of the column body (1.5 m) corresponds to about one half of the height of existing columns, which proved sufficient for not disturbing stress distribution in the connection area, as proven by numerical calculations.

The test setup includes definition of measurement locations (MM) for measuring displacement and relative deformation according to numerical calculation results (Figure 16.b). On an average, 15 LVDT (Linear Variable Differential Transformers) of variable base were used for measuring displacement (Figure 4). The stress distribution in column was obtained by measuring relative deformations using strain gauges placed along the column body (Figure 4). The secant modulus of elasticity ($E_0 = 62900$ MPa), obtained by experimental measurement [13] according to HRN EN 14580:2008, was used in the calculation. The measurement locations were divided into three groups (20 strain gauges on an average) along the column height: column top (VS), column mid-height (SS) and column bottom (DS), with the note that MM (measurement locations) were situated 10 cm away from contact surfaces. Such distribution proved sufficient for interpretation of stress distribution, with additional use of numerical models. At that, direct measurements on contact between column elements was avoided, as such measurements could disturb local distribution of stress. It should be noted that the test configuration has been continually improved [14] during the testing, especially after preliminary tests on similar concrete samples. An appropriate test setup adequate for approximation of column behaviour - involving use of appropriate numerical models - was obtained in the end, as will be shown below on appropriate test examples.

2.2. Existing laboratory tests without lead insert

Previous centric and eccentric tests, not involving the lead inlay, are described in paper [5]. Some special issues needed for analysing the role of the lead insert will be presented in this section (using sample K3 as an example), including some additional analyses. The testing of all samples started by applying a 100 kN force with the hydraulic cylinder centrally positioned above the column, which was named the test phase. At least a generally uniform stress distribution along the cross section (about 2.0 MPa) was expected in this phase. However, a pronouncedly non-uniform distribution of stress was in fact obtained despite stringent laboratory conditions, careful extraction, and accurate treatment of samples surfaces (Figure 5.b). This was also observed on all other samples [13].



Figure 4. Laboratory test setup illustrated by sample K5

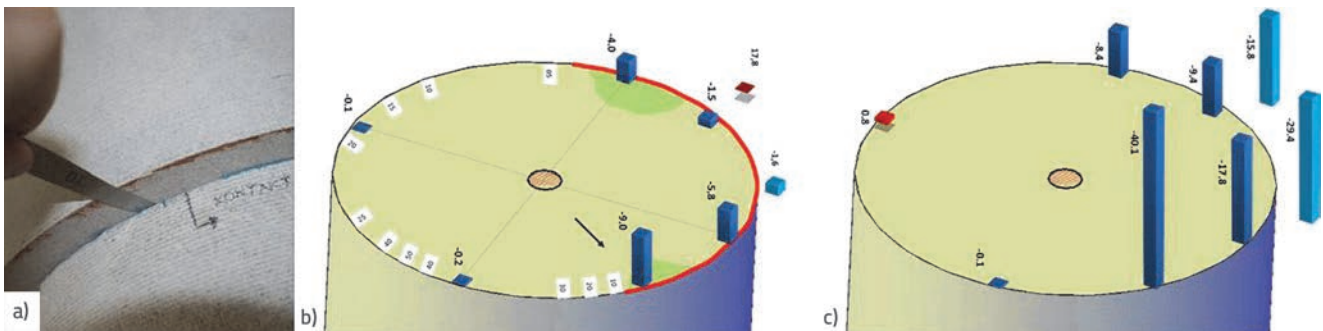


Figure 5. a) Determination of gaps by measurement sheets; b) Stress values at VS for test phase K3 [MPa]; c) Stress values at VS for central and eccentric load [5]

Due to such an unexpected behaviour, additional measurements had to be conducted so that the results can be interpreted, i.e. so that they can be related to the results of numerical modelling. One of these measurements involved determination of irregularities of contact surfaces. This measurement was conducted using the FaroArm device [15] and it was determined that roughness or irregular shape of contact surfaces amounts to less than 0.5 mm (the accuracy of the device is 2/100 mm). It was established that even such small values are sufficient to prevent uniform contact between column elements. This was further confirmed by additional measurement of gaps between contact surfaces on extracted specimen using measurement sheets (Figure 5.a). Values of gaps reached up to 1 mm (Figure 5.b), but it was crucial that the area of contact between column elements could be clearly defined (marked by red line in Figure 5.b). The described measurements contributed to interpretation of results from the testing phase, i.e. the areas of stress concentration corresponded to the areas determined by measurement sheets. It should be noted that samples sometimes additionally "adjust themselves" immediately following application of force. Furthermore, it is important to take into account irregularities at all contact surfaces (six in total), i.e. adjustment of samples in space, which ultimately results in some amount of eccentricity.

A three-dimensional schematic presentation of stress distribution, obtained by measurement of relative deformations in strain gauges, was selected for presentation of results, because it also shows stress relationships (compression stress is shown in blue colour, and tensile stress is shown in red). A rough estimate of the influence of irregularities can be obtained by comparing peak stress concentration values (about 9.0 MPa – Figure 5.b) with average stress in the case when the stress distribution along the cross-section is uniform (about 2.0 MPa). At that, it is important to take into account the fact that measurement points are situated 10 cm away from contact surfaces, so the values also contain stress distribution from the concentration zone at contact surfaces to measurement locations (at the column surface). A more accurate estimate of real stresses at contact surfaces can be obtained using numerical models (Figure 16.c), which also include measured gaps between contact surfaces. Usually, stress concentration values (at contact surfaces) are 2 to 3 times higher in numerical models compared to values at

measurement points (10 cm away from contact surface), which would mean that in the example given in Figure 5.b the greatest stress at the contact surface exceeds 20.0 MPa (ten times more than the expected value).

Numerical models enable good estimate of the areas of contact between column elements (surfaces) such as those given in Figure 5.b. (marked in green), but also of the stress distribution along the entire sample (Figure 16.c). Irregularities on contact, i.e. even the slightest gaps, means that the entire cross-section of the column will not be activated during the load transfer, but rather that small stress concentration areas will be formed. Concentrations of contact stresses actually caused the occurrence of first crack after application of force in a centrally placed hydraulic cylinder between 136 and 297 kN for all tested samples without lead insert. It is obvious that initial gaps during setting up of contact between elements cannot be solved in any other way, so stress concentrations eventually lead to crack opening. Due to reserves in bearing capacity, the column maintain its bearing capacity after redistribution of stresses (within the cross-section), but such fractured state can become dangerous due to action (superposition) of other loads (Section 2) and because fractured parts of the column may fall off.

The above mentioned effect is related to approximately centric load (centrally placed hydraulic cylinder), but usually much less favourable column behaviour arises from eccentric load (eccentrically placed hydraulic cylinder). The influence of eccentric load directly depends on irregularities between contact surfaces, as, during eccentric load, the capital normally exerts additional pressure in one of initially determined contact zones (areas), and causes pronounced stress concentrations. Depending on the initially realized concentrations, the eccentric load can lower the stress in the concentration zone, additionally increase stress concentration, or cause propagation of the existing fractures. It is significant to note that even a slight change in angle, i.e. from 0.003° to 0.2° causes pressure increase on one side of the cross-section (Figure 5.c) and development of high concentration, which very rapidly results in the opening of new fractures and, eventually, in complete failure of the column (typical behaviour of all samples). The eccentric load causes faster increase in stress, as can clearly be seen on the testing diagram (Figure 6) which also describes the overall course of testing for sample K3. The diagram presented in Figure 6 shows the values of centric load

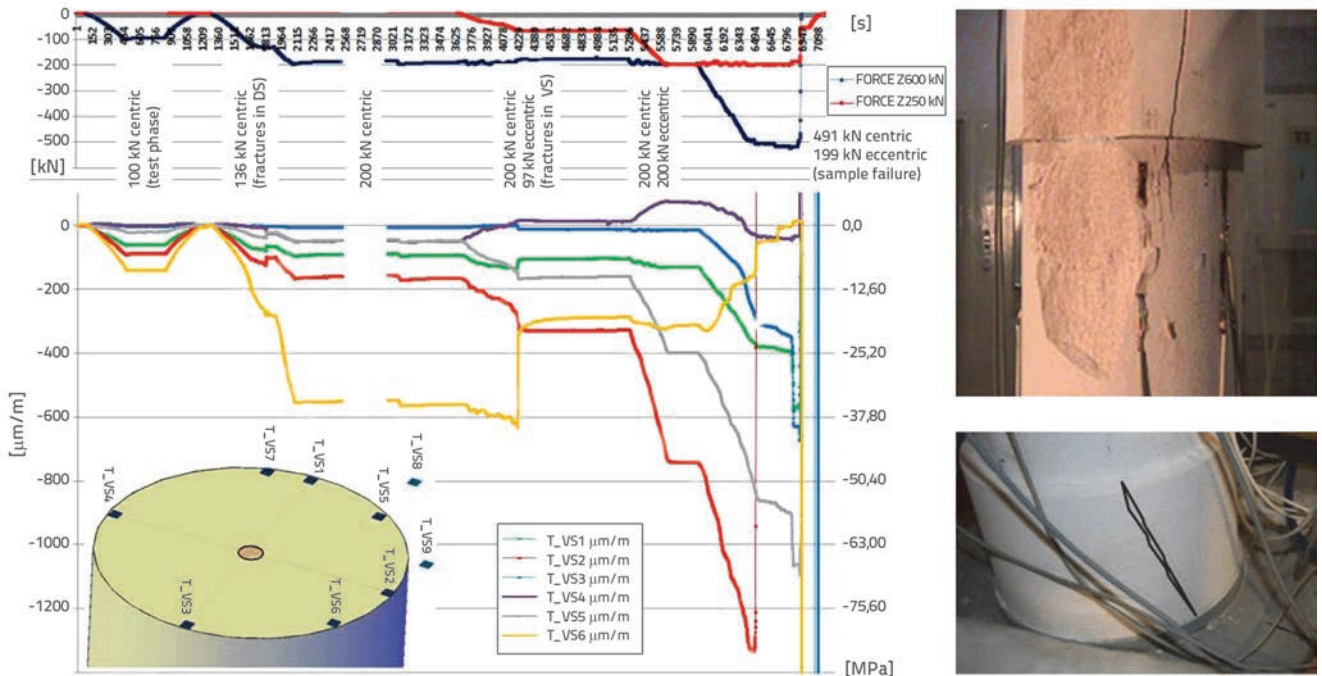


Figure 6. Testing diagram for sample K3 – relative deformation (stress) over time with presentation of load input for measurement locations at column top (VS), with photographs showing crack opening at VS and DS

(force Z600 – marked in blue) and eccentric load (force Z250 – marked in red), and also provides marks showing typical testing phases. Furthermore, the values of relative deformation are also presented (a set of values to the left) as well as the corresponding stress values (a set of values to the right) for measurement positions at the top of the column (VS) which are distributed according to the enclosed schematic. Changes at measurement locations can clearly be monitored on the testing diagram (Figure 6) as related to the level of load, e.g. opening of cracks, typical re-distribution of stress along cross-section (after crack opening) and, eventually, sample failure (Figure 7).

measurement point T_VS2 (expected zone of capital pressure at the edge of the column) show a clear influence of eccentric load and emphasize the zone in which the column failure finally occurred. It should be stressed that the distribution of measurement points in case of sample K3 slightly differs from the described test configuration, as it is adjusted to measurement of gaps between contact surfaces. Furthermore, at the analysis of results, it should be noted that the sample is already significantly cracked at final stages of the testing. A detailed analysis of test results for sample K3 is presented in paper [5].

When conducting tests for other samples, various loading methods were used in order to test influence of contact stresses on centric load (up to 500 kN in the centrally positioned hydraulic cylinder), combination of centric and eccentric load (200 kN in centrally positioned hydraulic cylinder and 200 kN in eccentrically positioned hydraulic cylinder), eccentric load only (up to 200 kN in the eccentrically positioned hydraulic cylinder), etc. All samples without the lead insert were considerably cracked or lost their bearing capacity at centric load of 500 kN and eccentric load of 200 kN (Figure 7). It should be noted that the centric force of 500 kN represents approximately 11 % of the ideal bearing capacity (bearing capacity of an ideal cross-section subjected to centric compression, assuming uniform distribution of stress), which approximately corresponds to the assumed utilisation of traditional stone columns (approximately 10%) [16]. In conclusion, the existing research shows that the problem with contact stresses is primarily caused by non-uniform stress distribution on column elements and is especially pronounced in case of eccentric load. It can be stated that it is a "structural deficiency," as emphasized by old builders. Therefore, the retrofit procedure must include solution for the two mentioned problems.



Figure 7. Samples K1, K2, K3 and K6 after failure

To illustrate, the results for the measurement point T_VS6 (point of the highest stress concentration for test phase) can also be monitored, where, the crack opening occurred already at centric load due to stress concentrations. In addition, the results for the

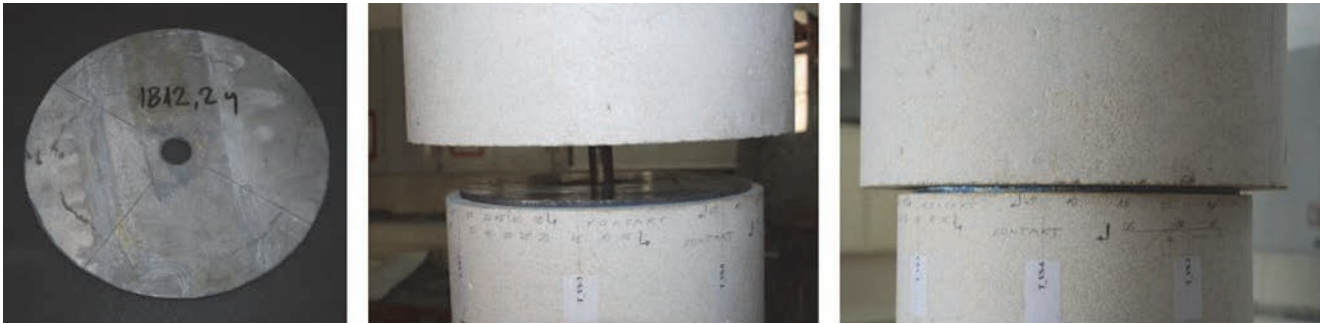


Figure 8. Lead inlay and its placing into column top for sample K5

2.3. Laboratory testing with lead insert

2.3.1. Testing sample with lead insert

The process of testing sample with lead insert will be described using sample K5 as an example. The testing itself was conducted based on the previously described test configuration. The lead insert 23 cm in diameter and 4 mm in thickness was placed between contact surfaces of column elements (Figure 8), i.e. as connection between the column body and the capital and base. It should be emphasized that the radius of the lead inlay is by 1 cm smaller than the column radius. The idea behind this is to ensure exertion of column pressure closer to the column axis (away from the edge itself) and to take into account the unknown behaviour of lead at such specific load, and at other loads such as temperature, cyclic load, etc. Smaller radius allows lead to extend and to adapt better to irregularities at contact surfaces, and the insert can be made invisible if requested (e.g. by historic preservationists). The usual measurement of gaps between elements using measurement sheets was not conducted because of the lead insert, but it was observed by visual inspection that the pressure at contact is uneven. The usual irregular distribution of stress was confirmed by results from the testing phase (Figure 9) in which two pronounced areas of pressure can be noted for VS at opposite sides of the cross-section, while pressure is dominant at one side of cross-section for DS. Stress values are lower compared to all other samples, which can be attributed to the role of the lead insert.

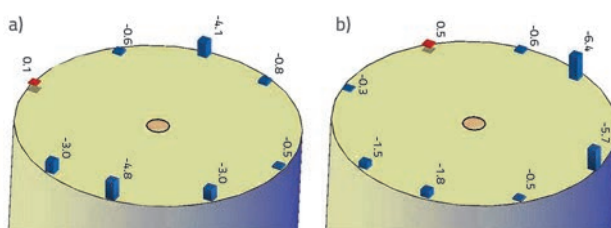


Figure 9. Testing phase for sample K5 with lead insert: a) stress at VS [MPa], b) stress at DS [MPa]

The testing was continued by applying load up to 500 kN (in the centrally positioned hydraulic cylinder) in order to determine the lead insert performance with regard to pressure exerted by column elements (irregularities of contact surfaces). The test

results (Figure 10) reveal a highly uniform distribution of stress compared to other samples [13], i.e. the zone of pronounced stress concentration cannot be distinguished. On top of that, numerical analysis results reveal that the stress distribution presented is possible only when there are four similar areas of support, which was not the case for other samples.

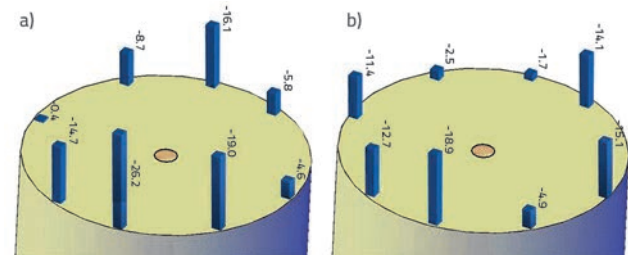


Figure 10. Testing phase at centric force of 500kN for sample K5 with lead insert: a) stress at VS [MPa], b) stress at DS [MPa]

"More regular" behaviour can also be observed at the testing diagram (Figure 11) where the stress increase at measurement locations is more uniform and less pronounced. The highest increase can be observed at the measurement point T_VS3, but this increase does not greatly differ from increase registered at other measurement locations. Such results can be attributed to the influence of the insert, i.e. it can be concluded that properties of the lead inlay have enabled the sample to adjust itself to irregularities of contact surfaces, but without cracking. The testing continued with application of eccentric load (using hydraulic cylinder at the mid-length of the steel beam), which caused the capital to press onto the edge of the column. The rotation of capital with respect to the axis could also be visually observed, and the results obtained at almost all measurement locations revealed a highly uniform re-distribution of stress toward the edge of cross section at VS (Figure 12.a). This was also confirmed by changes in relative deformations (stresses) at the testing diagram (Figure 11), where a relatively rapid increase of stress can be observed for measurement locations adjacent to the expected contact (T_VS2, T_VS5 and T_VS6), but also a pronounced regularity (compared to other samples) and a more uniform distribution of stress (to a wider area). A certain stagnation can be observed at the measurement location T_VS3, which was marked as critical with regard to centric load. This stagnation is due to the fact that the measurement

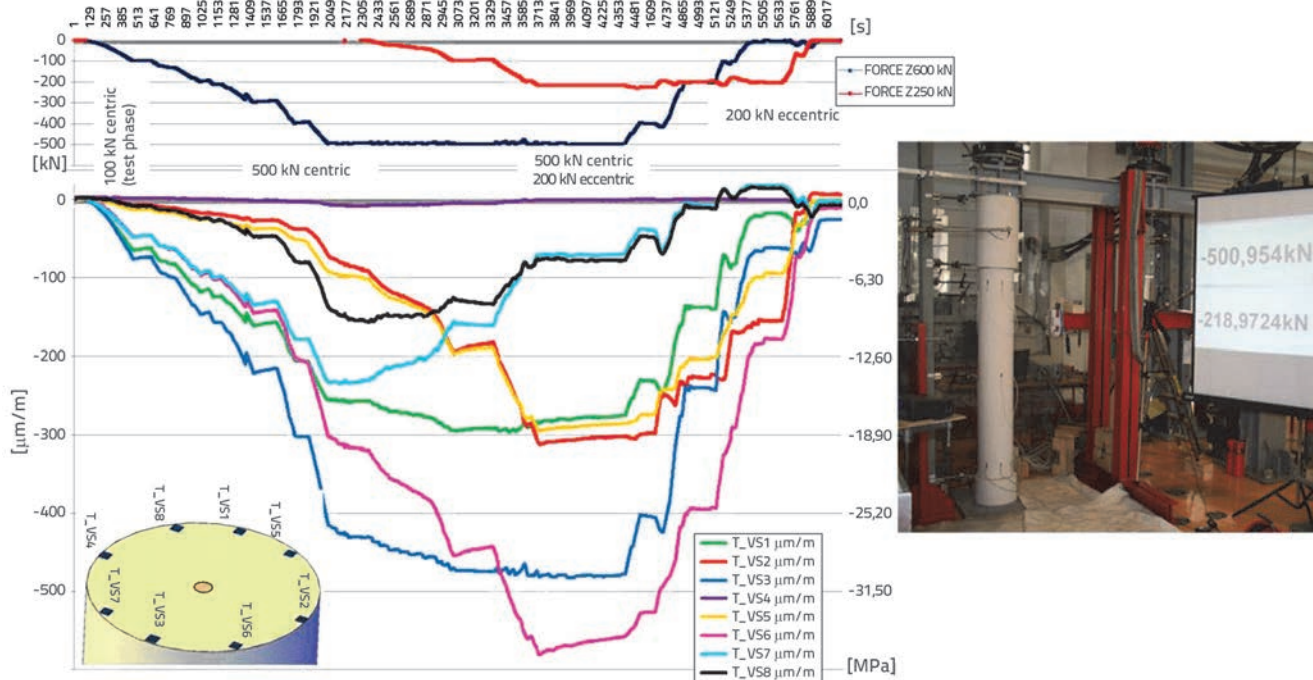


Figure 11. Testing diagram for sample K5 – relative deformations (stresses) over time, with load input for measurement point at column top (VS) and photograph of the final phase of testing

location is not situated in the vicinity of the expected contact. Results for column bottom (DS) reveal influence of eccentric load (Figure 12.b), but also the slight contribution of the sample "adjustment" in space due to irregularities of contact surfaces.

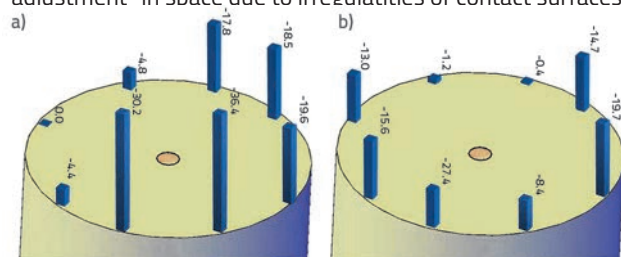


Figure 12. Testing phase at centric force of 500kN and eccentric force of 200kN for sample K5 with lead inlay: a) stress at VS [MPa], b) stress at DS [MPa]

It can be concluded that the lead insert ensures better column behaviour at eccentric load because of a larger contact area, especially as the insert was "pulled in" (its radius was smaller compared to column radius) and hence concentration at edge was prevented, and the contact area was "transferred" toward the centre of cross-section (toward the cross-section axis) to a larger area. A detailed analysis of results obtained at all measurement locations did not reveal any failure or redistribution of stress within the cross-section. In addition, visual inspection of sample after testing did not show any incidence of fracturing, which means that the sample was able to withstand maximum load exerted in hydraulic cylinders (Figure 11), i.e. the very loads that proved critical for other samples (Figure 7). The inspection of lead insert after testing revealed local

deformations along the entire surface and a pronounced dent that corresponds to the place where capital exerted pressure at the edge of the column. It is important to note that, due to eccentric load, the capital actually rotated with respect to the column body by only 0.17°, which corresponds to the values obtained for other samples [13], and is also in line with other research results [6]. In the scope of additional analysis at the last phase of testing, the column was subjected to eccentric load only (201.9 kN) at an angle of 0.362°, but the sample did not suffer any damage (Figure 11).

Finally, it can undoubtedly be confirmed that, because its properties (malleability in particular), the lead insert acts favourably (it adjusts to irregularities) by compensating irregularities at contact surfaces. In other words, it compensates for an uneven contact of column elements and enables greater contact surface. A similar conclusion can also be drawn for eccentric load, in which case a larger contact area is enabled during capital to column edge contact and, considering the applied forces, this compensation is sufficient to prevent significant stress concentrations that would otherwise cause fracturing.

2.3.2. Sample testing after removal of lead insert

The same sample (K5) was tested once again after removal of lead insert using the same testing setup (except for minor height adjustments due to removal of lead inlay). In addition, the same testing procedure was repeated by initial application of force amounting to 500 kN via a centrally positioned hydraulic cylinder. This testing was conducted to finally confirm the influence of lead insert, but also to confirm results of all

other tests in which stress concentration problems at contact surfaces were noted.

Two distinct areas of capital contact with the column body were distinguished already for the test phase based on the results obtained for the column top (VS), which is also typical for other samples without lead inlay. One point of contact is at the edge of the column (rapid stress increase), and the other is within the cross-section, which was also confirmed by numerical analyses. Two contact zones were also identified for the column bottom (DS) but, unlike VS, without pronounced stress concentrations (Figure 13.b). These zones of contact approximately correspond to gaps measured between contact surfaces (using measurement sheets), with a usual minor adjustment of sample after application of load.

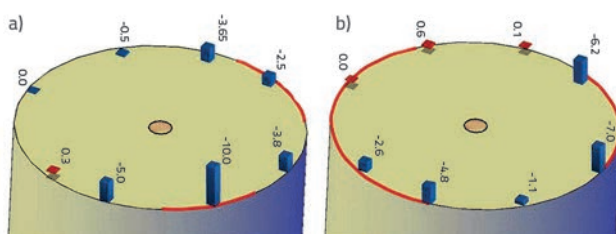


Figure 13. Test phase of testing for sample K5 without lead inlay: a) stress in VS [MPa], b) stress in DS [MPa]

The first visible crack opening (Figure 14) was visually observed at the base at a centric force of 287.9 kN, what can be also noticed on results at almost all measurement locations (especially at DS). A detailed analysis of numerical modelling results and experimental test results points to the conclusion that the top

of the crack occurred at the contact between the column body and the base. The crack opening was followed by usual stress re-distribution [5], primarily at the contact between the column body and the base, but this redistribution was also observed at measurement locations for VS (Figure 14), which is a usual behaviour caused by adjustment of the sample.

The testing was continued and sample splitting occurred at a centric force of 476.2 kN (Figure 14). At that point the testing was interrupted. The fracture opened almost along the middle of cross-section, and it was visible from both sides of the column (Figure 15). Lengthwise, it spread along more than one half of the column height. The fracture opening corresponds to measurement results for VS (Figure 14), i.e. they are a direct consequence of stress concentration near measurement locations T_VS3 and T_VS6 and near the location of contact within the column cross-section, which was observed at MM T_VS1, and confirmed by numerical calculations. The analysis of stress distribution prior to and after column splitting reveals redistribution within the cross-section, and shows that the sample maintained its balance by mostly leaning onto one side of the cross-section. It is important to note that each half of the split sample has a cross section area that is sufficient to bear centric load of 500 kN, i.e. it is possible that the sample will "find" a new leaning zone, i.e. a new state of balance for load bearing. Stress redistributions within the cross-section (after crack opening), by which the column maintains its bearing capacity until the full loss of stability, can be defined as typical behaviours, as they can be observed at all samples subjected to testing. Additional tests (not relevant for results presented) were made prior to sample dismantling. During these additional

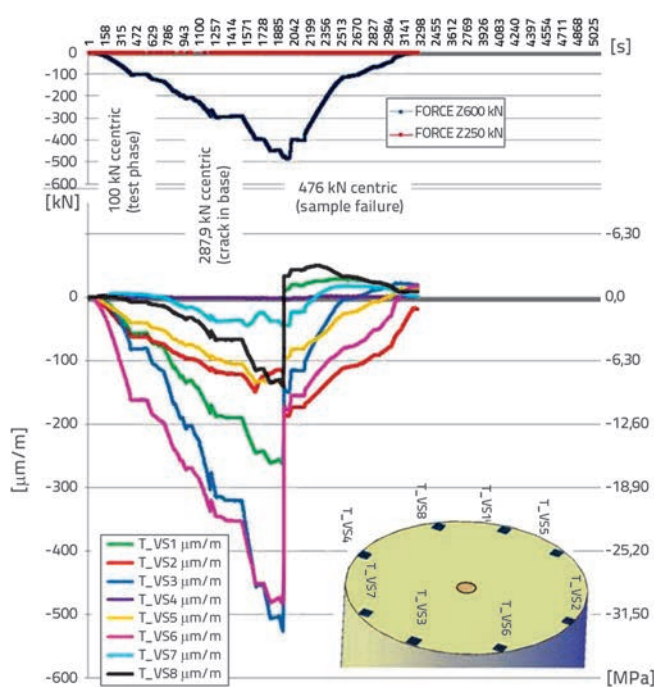


Figure 14. Test diagram for sample K5 (without lead insert) – relative deformations over time with application of load at measurement for column top (VS) and with crack opening photos for VS and base

tests, the column body was fully split in the end, but the same was observed for column base in the direction of the crack that opened the first (Figure 15). Finally, after removal of lead inlay, significant stress concentrations (with rapid stress increase) were observed at contact surfaces that caused crack opening and, eventually, failure of the sample.

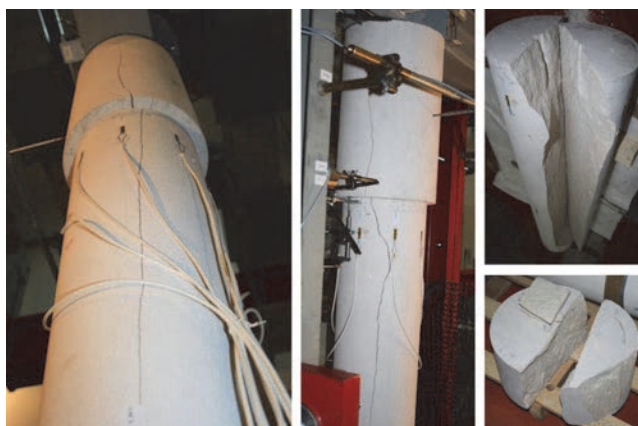


Figure 15. Crack on both sides of sample K5 without lead inlay, and column body and base splitting after sample dismantling

3. Numerical analyses

3.1. Numerical approaches to the problem

Numerical analyses are crucial for the interpretation of laboratory testing results, approximation of connections behaviour and cracked state and, finally, for assessment of the structural bearing capacity. In addition, numerical analyses have played a principal role in the initial identification of connections deficiencies [6] when subjected to eccentric load, which has spurred more detailed investigations. This section provides an insight into preliminary numerical testing of the influence of lead inlays on the bearing capacity of traditional columns. The models and results presented in this paper are a part of an extensive investigation, which is why various numerical

approaches applied so far will briefly be described in the beginning of the section.

Causes of problems with traditional columns are identified by a numerical model of the atrium of the Rector's Palace in Dubrovnik (Figure 16.a) created in program packages FEAP 7.4 [17] and GID 6.1.2a [18], which were additionally extended to exclude overstressed finite elements. This contributed to better description of behaviour in the vicinity of connections [6]. Recent numerical analyses were more oriented toward modelling the connection itself using models of varying complexity, through which investigation results were linked with the existing structures [19].

Ever since the early planning and testing phases, laboratory tests have been supported by models created using the software SAP2000 [15]. The laboratory testing model (Figure 16.b) is described in full detail in paper [5]. This model was ultimately used for the verification of testing, interpretation of results, and calibration of global models. It is important to note that the behaviour of connection, i.e. relative rotation between column elements (modelled by brick elements) and contact with one side of the cross-section, was successfully modelled by adjustment of elements within the SAP program package. The described non-linear behaviour was defined by the link elements between model nodes (contact surfaces) according to the theoretical basis defined by Wen (1976) and by Park, Wen and Ang (1986), and further elaborated by Nagarajah, Reinhorn and Constantinou [20]. Typical distribution of stress at the contact between capital and column edge is presented in Figure 16.c. The results show concentration of compression trajectories at the edge of the cross-section (nuances of blue colour), and distribution of stress from the area of concentration on contact surfaces to the measurement points. The subsequently discovered problem of uneven connection of contact surfaces was taken into account by the models so that the properties of connection elements also included measured deviations (distances between contact surfaces). This was crucial for a more accurate approximation of connection behaviour, and for interpretation of test results. As emphasized

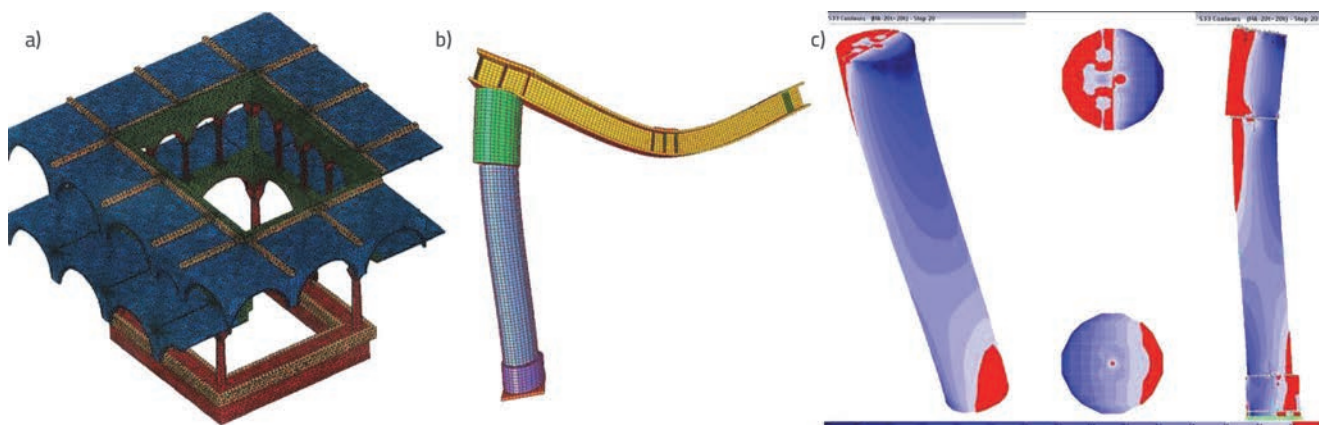


Figure 16. a) Numerical model of the Rector's Palace [10]; b) Numerical model of testing – deformed state at eccentric load [19]; c) Stress distribution along column shaft, contact surfaces, and in vertical cross section through column axis [5]

in the previous section, accurate values of stress concentration at contact surfaces cannot be obtained by relative deformation measurements. However, a highly reliable extrapolation can be made using well calibrated numerical models.

It is important to emphasize that the results of the model with brick elements and links confirm the need for using more detailed models in order to obtain a realistic description of column behaviour [5]. However, the column behaviour was adequately approximated by the described model during the experiment, but only for initial phases of testing. The next phase of numerical research involves formation of a numerical model that can monitor the process of opening and development of cracks in stone. Some relevant results will be presented below, with an emphasis on numerical analyses that have confirmed satisfactory use of the lead inlay.

3.2. Numerical testing of sample with the lead inserts

3.2.1. Description of numerical model

Numerical computations and results obtained in the scope of a wider research are presented in this section. The development of cracks on contact surfaces due to centric and eccentric loading of stone blocks will be presented, and favourable effects of lead inlay will be analysed in detail. The analyses were conducted using the program package Abaqus Standard. Due to considerable complexity of the model, only results obtained on the test sample that approximates sufficiently well the described typical behaviour will be presented in the following text. The test sample is formed of two cylinder-shaped stone blocks, measuring 25 cm in diameter and 15 cm in height (Figure 17). The model is smaller compared to laboratory samples due to high complexity of failure mechanism. In fact, the basic objective is to qualitatively present the mode of failure and the influence of lead inlay. Numerical verifications were made on two basic model types. In the first one, the connection between two blocks was realized by direct contact between two uneven surfaces, while in the second model type a lead inlay 10 mm in thickness and 25 cm in diameter was placed between uneven surfaces. Considerable effort was made to realistically describe unevenness of contact surfaces. Therefore, the surfaces were artificially defined by cutting one piece with irregular surface (Figure 17.a). As two cut blocks perfectly correspond to one another, the non-uniform contact was obtained by rotation of

the top stone around the longitudinal axis for a specified angle (15° , 30° , 45°). The highest deviation between contact surfaces amounted to 2 mm, which is more than the values obtained in laboratory.

The concrete damage plasticity (CDP) model in the program package Abaqus (based on the finite element method), was used as the stone material model. This model properly describes stone behaviour when subjected to static load and it is capable of defining sufficiently well (considering the available data) failure mechanisms of the system composed of two stone blocks in a complex stress state. The extended finite element analysis (XFEM) approach, as well as various material models based on brittle failure, were applied in the test phase of model preparation. Nevertheless, it was established that their use is not applicable in case of very complex state of stress in which the pressure localized in a small area is dominant. In addition, the CDP model has been properly tested and documented on unreinforced concrete elements, exhibiting behaviour relatively similar to stone. Additionally, samples made of unreinforced concrete were used in preliminary experiments [13].

Two types of failure mechanisms are assumed in the material model of stone (CDP), i.e. tensile cracking and the crushing of material subjected to compression (shear softening is not taken into account). In compression, the relation between stress and strain is linear until the stress value of σ_{c0} , which represents initial failure. This is followed by hardening until maximum stress σ_{cu} , and then by material softening. The behaviour of material at uniaxial compression outside of the elastic area is defined by inelastic strain ε_{cin} , which is calculated as the total deformation reduced by the value of elastic strain of undamaged material $\varepsilon_{cin} = \varepsilon_c - \varepsilon_{o\text{cel}}$, where $\varepsilon_{o\text{cel}} = \sigma_c / E_0$. In case of tensile stress, the model follows the linear relation until failure σ_{to} , which corresponds to crack opening in the material. After that, softening with the localisation of strain in the element follows. Behaviour in cracked state involves definition of post-critical stress as a function dependent on cracking strain ε_{tck} . The cracking strain is defined as the total strain reduced for elastic deformation of an undamaged material $\varepsilon_{tck} = \varepsilon_t - \varepsilon_{o\text{tel}}$, where $\varepsilon_{o\text{tel}} = \sigma_t / E_0$. The tensile behaviour in softening region of a material can be described by the stress-strain relation, or by the fracture energy cracking criterion. The first approach can cause excessive sensitivity of the mesh in case of materials exhibiting highly unstable post-critical behaviour. In this research, the fracture energy approach was used, which is the energy required to open a unit area of



Figure 17. a) Sample geometry and irregularities at contact surfaces, b) numerical model of the sample

crack and it represents a material property (area of post-critical region of the $\sigma - \epsilon$ curve). Laboratory testing has revealed fracture energy of 0.1 J in stone samples. The yield function was defined according to Lubliner [21] and modified according to Lee and Fenves [22] taking into account difference in behaviour at compression and tension. The evolution of the yield surface is controlled by hardening variables ϵ_{tpl} and ϵ_{cpt} that are linked with the tensile or compressive state of stress. Basic material model data were obtained by laboratory testing of stone samples, during which the elastic modulus ($E_0 = 62900$ MPa), tensile strength ($\sigma_t = 17$ MPa), and compressive strength ($\sigma_c = 92$ MPa) were determined. The elastoplastic material model of lead was assumed. The behaviour is linearly elastic until yield point, and it is determined by the elastic modulus $E = 16000$ MPa, Poisson ratio $\nu = 0.44$, and yielding $f_y = 10.2$ MPa. The post-critical behaviour is defined by the relation between the stress and plastic strain. It should be noted that this model does not fully describe lead behaviour in a highly complex state of stress, with very high plastic deformations of material in compression, i.e. in such instances the lead creep phenomenon at long-term load is not taken into account.

Properties related to the contact between stone blocks are defined in both tangential and normal directions. In tangential direction, the friction coefficient amounting to 0.2 was assumed, and the penalty formulation of kinematic constraint was applied. On the other hand, a rigid contact with possible detachment of surfaces is assumed in normal direction. Models with inlays also involve definition of properties of the contact between the stone and the lead inlay, with possible detachment of contact surfaces, and without possibility of one material penetrating into another.

The finite element mesh is formed of approximately equal regularly shaped hexahedrons (Figure 17.b). Elements are approximately 10 mm in length, and the mesh is adjusted to material behaviour in the post-critical tensile area, in which the system is unstable and becomes sensitive to the mesh size. The calculation was conducted in two phases. The initial adjustment of stone blocks is modelled in the first phase in which the top block is freely lowered onto the bottom block.

Normally, the contact between the blocks is realised at three to four points, which corresponds to measurement results, and depends on the level of irregularity of contact surfaces. As no boundary condition has been defined for the top block, it can be freely placed onto the bottom block to achieve static equilibrium. A forced displacement of a point located at the top of the top block, which is by 50 mm eccentric to the block axis, is induced in the second phase. The numerical calculation is conducted using the Newton-Raphson method with controlled displacement, in which the problem is analysed as a staticone. The maximum increment is 0.01 and the minimum size is 10^{-13} , as required for calculations in unstable (tensile) areas after crack opening. Typical model results with and without lead, and the analysis of results for the test model described, are presented below. Additional development of the model is planned in subsequent phases of research. It should be noted that, despite the mentioned limitations of the test model, the results actually correspond to typical behaviour observed during experimental testing.

3.2.2. Results – model without lead

Calculation results presented in this section are related to typical loading phases. The cracking pattern is presented through maximum principal plastic strain (PE). Contact points after establishment of contact between the top and bottom stone blocks are shown in Figure 18.a, where an initial contact in four points can be observed. Due to increase in eccentric load (second phase), the stress is concentrated in points situated in the zone in which the force is applied. Figure 18.b shows positions of initial cracks at the bottom stone block, which correspond to the stress concentration points. The crack opening direction is mostly radial and, over time, the cracks gradually propagate and start to connect with one another. A moment prior to system failure is shown in Figure 18.c, where the zone to be detached can be observed. This is followed by failure with pronouncedly unstable post-critical behaviour.

The described phases can be seen in Figure 19 on the force-displacement diagram for the force application point. The diagram is divided into two typical areas (two loading phases).

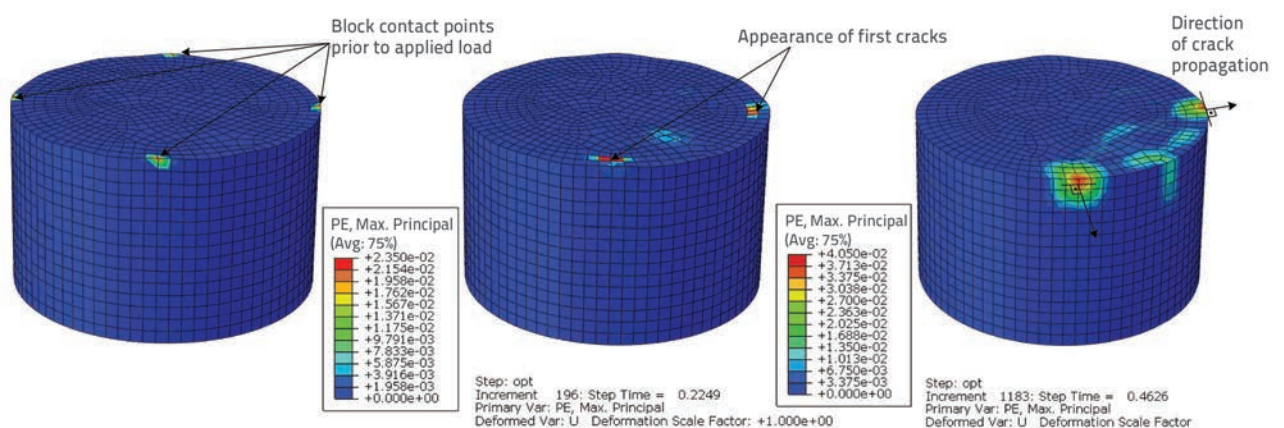


Figure 18. a) Points of initial contact between blocks; b) Plastic strain at the start of eccentric load; c) Plastic strain a moment before failure

The first area is the zone in which the contact between surfaces has been realised, and the second area is the phase of eccentric load of the top stone block. According to the previously described process, the bearing capacity is achieved in the moment of $t = 0.47$ of the second phase (marked in the figure); it is the pseudo-time that represents a calculation increment (without any physical meaning). Additionally, the loading scheme is presented, and the failure surface of the stone sample (end of phase 2) is also marked.

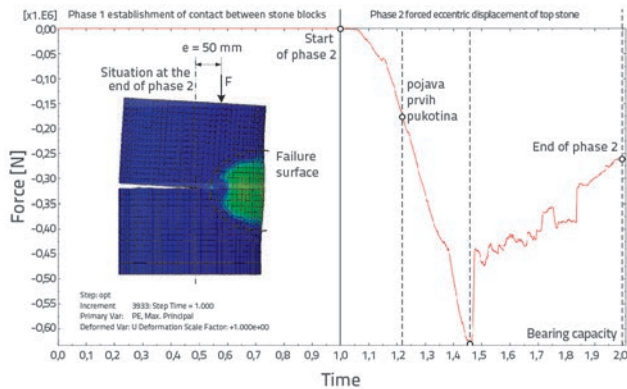


Figure 19. Diagram of force and pseudo-time on sample without lead inlay

3.2.3. Results – model with lead

The sample with lead inlay in between the stone blocks is analysed according to the same scenario. Figure 20.a shows the area of contact between the lead and the stone at the force equalling approximately 40 % of bearing capacity. It can be observed that there is no local concentration of load at the edge, but rather a redistribution to a wider area. Although the area of force transfer can still be observed, it is no longer localised. Figure 20.b shows the area of the opening and development of

cracks, and subsequent gradual formation of a failure surface. The crack opening is accompanied by stress relaxation, and so further development of cracks is slowed down. This enables favourable distribution of stresses in critical cross-section in time until formation of the surface failure (Figure 20.c). This point is marked by sudden stone block failure. The direction of crack development (detachment) is perpendicular to the failure surface. The stress relaxation is enabled by yielding of the lead inlay in maximum stress zones. All these loading phases can be seen in Figure 21. It can easily be observed that the failure surface is unsymmetrical compared to the lead inlay, which is caused by the difference in boundary conditions between the bottom stone sample (fixed) and top stone sample (free rotation about both horizontal axes through the point of force application). The initial distribution of stress is similar but, due to unfavourable position of failure surfaces, it occurs in the bottom sample. The bearing capacity is achieved in the moment $t = 0.67$ (of the second phase) and it should be noted that it is approximately two times greater compared to the sample without lead. A pronouncedly unstable post-critical area and sudden drop in bearing capacity after failure can be seen in the diagrams.

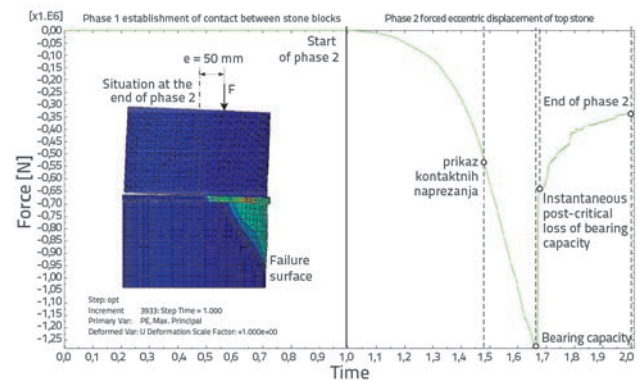


Figure 21. Diagram of force and pseudo-time for sample with lead inlay

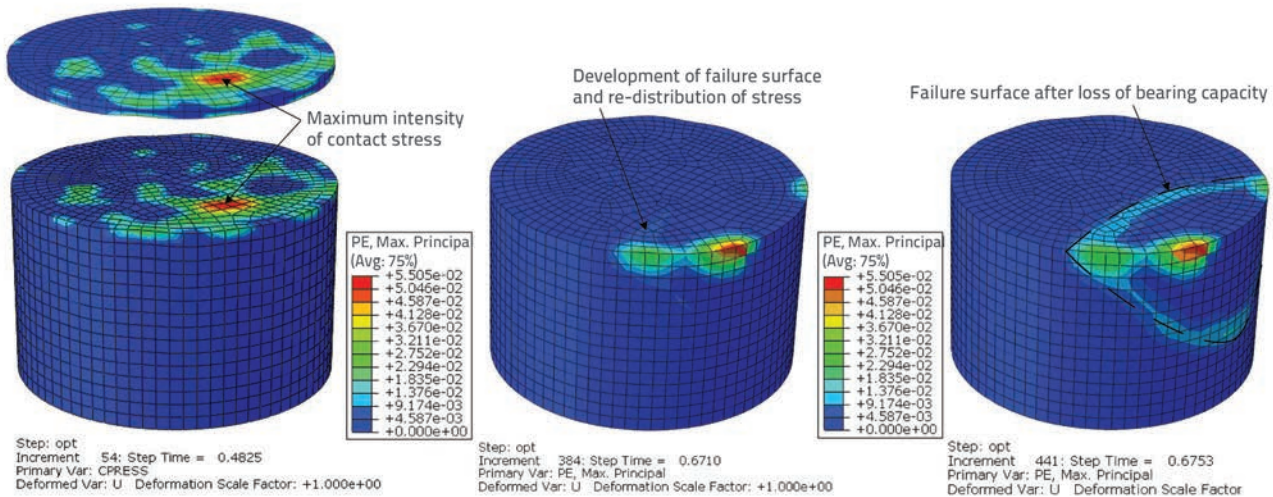


Figure 20. a) Zone of contact stresses between stone surfaces; b) Main plastic tensile strain immediately before failure; c) Main plastic tensile strain a moment after failure

3.3. Analysis of results

Figure 22 shows comparison of equilibrium curves of the numerical models with and without lead inlays. The calculation was made for different positions of contacts surfaces, which was realized by rotation of the top part of the model about the vertical axis for an appropriate angle (15°, 30° and 45°). Each position results in different contacts between stone blocks, i.e. in a different distribution of stress concentrations. However, a common feature to all models without the lead inlay is the concentration of stress in the local (small) area and rapid opening of cracks. By increasing the load, cracks continue to develop and cause failure without an increase in load, which results in a relatively low bearing capacity. Unlike the described behaviour, the use of lead inlay (as a "buffer zone") enables considerable reduction in contact stresses, i.e. the stress is redistributed to include areas that were initially not in contact. By increasing the load, the lead is in the state of yielding and is hence able to transfer load more uniformly from the top stone to the bottom stone. One of the consequences of stress relaxation in cracks is the redistribution of stress to other areas of the contact surface, which ensures a much greater bearing capacity of blocks.

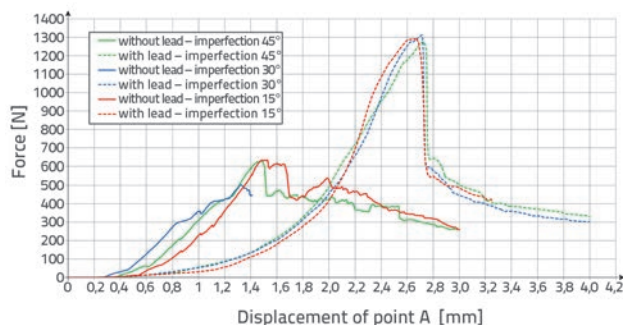


Figure 22. Force – displacement diagram for blocks with and without inlay, with eccentric load

In the presented example, the bearing capacity of blocks with lead inlay is by approximately two times larger compared to the model without the inlay. An additional advantage is that highly uniform bearing capacities for various contact positions (depending on the angle of rotation of the top stone) are

obtained by using the lead inlay, which leads to the conclusion that irregular contact surfaces (which are unknown) do not greatly affect the bearing capacity of the system (for the case with lead inlay). It should be noted that presented results are relevant only for the irregularities measuring approximately 2 mm, although similar behaviour can be assumed for smaller irregularities as well.

4. Discussion

The analysis of results for the column without the lead insert shows that first fractures appear at centric force values (centrically placed hydraulic cylinder) of 136 to 297 kN. For comparison, it should be noted that failure occurred at the force values of approximately 240 kN during the compressive strength testing on cubes measuring 5.0 x 5.0 x 5.0 cm [13]. It should also be noted that axial force of approximately 200 kN was obtained by experimental measurements and numerical analyses of cracked columns of the Rector's Palace in Dubrovnik (which initiated this research). It is clear that the problem involving irregularity of surfaces and uneven contact causes high stress concentrations which eventually lead to the formation of fractures.

For samples tested in laboratory, the treatment of contact areas was conducted with an accuracy of approximately 0.5 mm, which was confirmed by laboratory measurements. This accuracy is in accordance with recommendations given in stone-related standards, although it should be noted that the standards do not set limitations with regard to this problem of contacts. If the level of treatment is compared with manual procedures, i.e. with values that could have been obtained by ancient builders, it can be reasonably assumed that the problem is actually even more pronounced. Manual treatment of contact areas results in local deviations (Figure 23), which depend on tools used in the treatment (and these tools have been changing over time), and on the level of expertise and experience of the builder. It is also important to take into consideration geological age, mineralogical composition, various physical properties, and structure or texture of stone but, considering high frequency of cracking of traditional columns built of various types of stone, it could be stated that the problem is of rather general nature. This has also been confirmed by various retrofit strategies throughout human history using

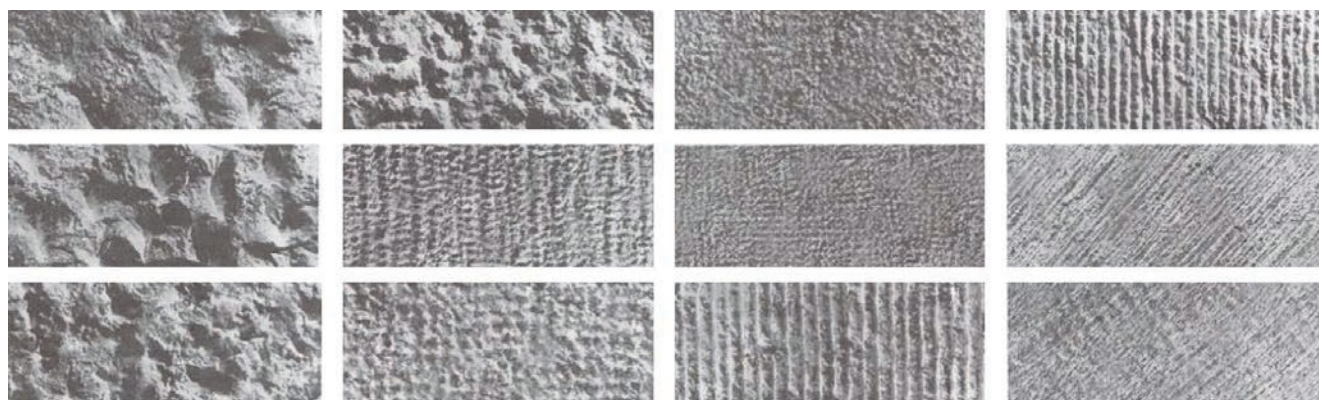


Figure 23. Appearance of stone surface during manual treatment of stone [23]

various types of mortars, stone dust and similar materials, in the construction of various types of columns.

Retrofit with lead insert placed in between contact surfaces reduces unfavourable influence of irregularity of contact surfaces, i.e. thanks to its properties this material enables better positioning of column elements and prevents stress concentration, as confirmed by laboratory and numerical analyses. The insert 4 mm thick was selected for laboratory testing. This thickness is sufficient for compensating irregularities and influence of eccentric load, i.e. rotation of capital with regard to the column body. The eccentric load (eccentricity of thrust line) has an additional negative impact in historic structures (for numerous reasons), as has also been confirmed by this study. It should be noted that inlay thickness must be determined based on properties of individual structures, i.e. based on amounts of centric and eccentric load, stone properties, column dimensions, shape of the load bearing structure, etc. In addition, it is recommended to test the impact of inlay on other parts of the structure, as improvement on one part of the structure, may cause difficulties on other parts.

5. Conclusion

According to research results, it can be concluded that problems with traditional columns start immediately after column erection, as initial stress concentrations develop at contact surfaces, because a uniform contact (stress distribution) is difficult to achieve due to irregularities on contact surfaces. At the end of construction work, a relative rotation of column elements and additional increase in stress concentration occurs by forming of a thrust line, which is always – at least to some extent – eccentric. When numerous unfavourable influences on a structure during its service life are added (differential settlements, earthquakes, changes in temperature, etc.), which are likely to additionally increase the eccentricity of thrust line, and as specific materials such as stone are susceptible to cracking, the fact that many traditional columns are fractured is hardly surprising. However, traditional columns have relatively high reserves in bearing capacity, and equilibrium is maintained through redistribution of stress, but it is important to note that such re-distributions are limited to cross-section of elements only.

According to results obtained during this research, lead insert has a favourable influence on the problems of irregularities of

contact areas and eccentric load, i.e. because of its properties, this insert reduces structural deficiencies of traditional columns. The deformation and penetration of lead inlay into irregularities of contact surfaces provides a better contact between column elements, i.e. the contact zone is increased and hence also the load bearing capacity of the system. These conclusions are confirmed by laboratory testing, and numerical calculations. The results also correspond to other research of the existing structures, which proves that this approach can be considered as appropriate for retrofit of historic structures affected by similar problems. It should however be noted that the tests conducted in the scope of this research were made with one type of stone (except for concrete samples) and based on a single experimental setup. In addition, the lead sample was not tested to long-term or cyclical loading, nor to various atmospheric conditions (such as changes in temperature), which was compensated in this study by the use of a smaller lead insert compared to the column radius.

The retrofit approach involving installation of lead insert belongs to traditional retrofit methods. The procedure is reversible, and can be made almost invisible. Nevertheless, this is just one retrofit possibility that can be modernized, accounting for state-of-the-art advancements. The principal aim of retrofit of historic structures is to preserve their integrity in original form. However, in case of traditional columns we are faced with a structural deficiency that systematically damages load-bearing elements of the structure and therefore, it is not worth preserving. The lead insert can be used to appropriately compensate for such structural deficiencies, while keeping the idea and original concept of the bearing structure.

Acknowledgements

The authors gratefully acknowledge the support of professor Damir Lazarević Ph.D. whose initial observations and research have initiated this study. Acknowledgements are also extended to Mr. Andro Fabres for his assistance in the preparation of test samples and to their colleagues: Joško Krolo, Domagoj Damjanović, Kelković brothers, Bojan Milovanović, Ivan Duvnjak, Marko Bartolac, Miro Matuzić and Zvezdana Matuzić and their undivided help in the conduct of experimental tests. The paper was funded by the Croatian Science Foundation through the project IP 2014-09-2899.

REFERENCES

- [1] Steinman, V.: Istražni radovi na Kneževu dvoru u Dubrovniku s načelnim prijedlozima sanacije, Knjiga II, Institut građevinarstva Hrvatske, Zagreb, 1974.
- [2] Lokošek, E., Kleiner, I.: Zamjena kamenih stupova u prizemlju dvorca Veliki Tabor, *Građevinar*, 56 (2004) 5, pp. 267-276.
- [3] Meli, R., Sanchez-Ramirez, A. R.: Structural aspects of the rehabilitation of the Mexico City Cathedral, International Seminar on Structural Analysis of Historical Constructions. Possibilities of numerical and experimental techniques, Barcelona, pp. 123-140, 1997.
- [4] Drosos, V.A., Anastasopoulos, I.: Experimental investigation of the seismic response of classical temple columns, *Bull Earthquake Eng*, 13 (2015) 1, pp. 299-310, <https://doi.org/10.1007/s10518-014-9608-y>

- [5] Atalić, J., Uroš, M., Šavor Novak, M.: Influence of contact stresses on bearing capacity of traditional stone columns, *Građevinar* 64, (2012) 11, pp. 891-903.
- [6] Lazarević, D., Dvornik, J., Fresl, K.: Analiza oštećenja atrija Kneževa dvora u Dubrovniku, *Građevinar* 56 (2004) 10, pp. 601-612.
- [7] Lazarević, D., Atalić, J., Fresl, K.: Reconstruction of Rector's Palace atrium in Dubrovnik: a key role of column connections. *Structural Studies, Repairs and Maintenance of Heritage Architecture XI*, eds. Brebbia, WIT Press, Southampton, pp. 289-303, 2009.
- [8] Vitruvius, P.M.: *De Architectura libri decem*, IGH, Zagreb, 1997.
- [9] Cakir, F., Kocycigit, F.: Architectural and structural analysis of historical structures, *Građevinar*, 68 (2016) 7, pp. 571-580, <https://doi.org/10.14256/JCE.1182.2014>
- [10] Atalić, J., Lazarević, D., Fresl, K.: Influence of Rotational Stiffness between Column Elements on Global Stability of Historical Constructions, *Proc. of the 8th European Conference on Research for Protection, Conservation and Enhancement of Cultural Heritage*, Ljubljana, pp. 60-62, 2008.
- [11] Roca, P., Gonzales, J. L.: A summary of the opinions put forward during the discussions, *International Seminar on Structural Analysis of Historical Constructions. Possibilities of numerical and experimental techniques*, Barcelona, pp. 394-407, 1997.
- [12] Buzov, A., Radnić, J., Grgić, N., Baloević, G.: Effect of the joint type on the bearing capacity of a multi-drum column under static load, *International Journal of Architectural Heritage*, 12 (2018) 1, pp. 137-152, <https://doi.org/10.1080/15583058.2017.1396380>.
- [13] Atalić, J.: Utjecaj kontaktnih naprezanja na nosivost tradicijskih kamenih stupova, *Doktorski rad*, Građevinski fakultet, Sveučilište u Zagrebu, Zagreb, 2011.
- [14] Lazarević, D., Atalić, J., Krolo, J., Uroš, M., Šavor, M.: Experimental and Numerical Analysis of Traditional Column Connections with the Possible Retrofit Concept, *Advanced Materials Research*, 133-134 (2010), pp. 479-484, <https://doi.org/10.4028/www.scientific.net/AMR.133-134.479>
- [15] FaroArm - Overview, www.faro.com, 1.6.2012.
- [16] Heyman, J.: *The Stone Skeleton*, Cambridge Univ. Press 1995.
- [17] Taylor, R.L.: *FEAP – A Finite Element Analysis Program*, Version 7.3, Programmer Manual, Department of Civil and Environmental Engineering, University of California, Berkley, 2001.
- [18] GiD, *The universal, adaptive and user friendly pre and post processing system for computer analysis in science and engineering*, Version 6, Reference Manual, CIMNE, Barcelona, 2000.
- [19] Atalić, J., Lazarević, D., Šavor, M.: Traditional column connections with iron dowels - experimental and numerical analysis, *Proceedings of the International Conference on Structural Analysis of Historical Constructions, SAHC2012*, Wroclaw, pp. 619-627, 2012.
- [20] *SAP2000, Integrated Software for Structural Analysis and Design*, Analysis reference manual, CSI: Berkeley, 2002.
- [21] Lubliner, J., Oliver, J., Oller, S., Onate, E.: A Plastic-Damage Model for Concrete, *International Journal of Solids and Structures*, 25 (1989) 2, pp. 299-329, [https://doi.org/10.1016/0020-7683\(89\)90050-4](https://doi.org/10.1016/0020-7683(89)90050-4).
- [22] Lee, J., Fenves, G.L.: Plastic-Damage Model for Cyclic Loading of Concrete Structures, *Journal of Engineering Mechanics*, 124 (1998) 8, pp. 892-900, [https://doi.org/10.1061/\(ASCE\)0733-9399\(1998\)124:8\(892\)](https://doi.org/10.1061/(ASCE)0733-9399(1998)124:8(892))
- [23] Crnković, B., Šarić, L.J.: *Građenje prirodnim kamenom*, IGH, Zagreb, 2003.